

Competition between charge- and spin-density waves in transition-metal dichalcogenides*

P. D. Antoniou

Department of Physics and The James Franck Institute, The University of Chicago, Chicago, Illinois 60637

(Received 25 July 1978)

We examine the consequences of competition between charge and spin-density waves in impure transition-metal dichalcogenides within the context of a Landau-Ginzburg mean-field theory. Magnetic impurities enhance a stable spin-density wave and stabilize an unstable one, while tending at the same time to suppress the charge-density wave. The formation of the spin-density wave is used to explain features of the magnetization, Hall-effect, resistivity, and negative magnetoresistance data for iron-doped TaSe₂. Randomness in the impurity position leads to randomness in the phase and amplitude of the spin-density wave, giving rise to a novel kind of spin glass, which we call a "spin-density-wave glass" and which, in this particular material, occurs against the background of a smeared charge-density wave.

I. INTRODUCTION

The physical properties of iron alloys of the layer-structured transition-metal dichalcogenides are extremely sensitive to the iron concentration. Transport properties such as resistivity, magnetoresistance, Hall-effect and superconductivity exhibit anomalous and in many occasions dramatic changes for iron concentrations in the 0–10% range.^{1–6} Susceptibility measurements⁷ also reveal a high degree of sensitivity to the iron concentration. In the case of excess iron intercalated into 2H-TaSe₂, the observed anomalies include a low-temperature resistivity minimum¹ and susceptibility maximum,⁷ negative magnetoresistance,¹ and anomalous behavior of the Hall coefficient as a function of both the temperature and the applied magnetic field.^{1,2} Superconductivity has not been studied for 2H-Fe_xTaSe₂ due to the very low transition temperature of pure 2H-TaSe₂ ($T_c = 0.2$ °K).⁸ Magnetic impurities, however, rapidly suppress superconductivity in 2H-Fe_xNbSe₂, which behaves somewhat similarly to 2H-Fe_xTaSe₂.^{5,6}

Pure 2H-TaSe₂ has been studied both experimentally and theoretically.^{9–24} The anomalous behavior of its properties such as specific heat, resistivity, and magnetic susceptibility has been attributed to formation of charge-density waves (CDW).¹⁸ A charge-density wave is a periodic variation in conduction-electron density of wave vector \vec{p}_1 arising, for example, from nesting of parallel portions of the Fermi surface. If there is no vector or rational fraction of a vector of the reciprocal lattice equal to \vec{p}_1 , the corresponding CDW is called incommensurate (ICDW); in the opposite case, it is called commensurate. The new periodicity introduced by the CDW breaks up the Brillouin zone and opens up gaps at the

new band edges. The occupied states move to lower energies, providing the reduction of the electronic energy necessary to stabilize the distortion. The resistivity minimum, the specific-heat peak, and the drop in the susceptibility below the transition temperature are associated with the opening of these gaps and the corresponding reduction of the Fermi surface. The trigonal prismatic 2H-TaSe₂ undergoes a second-order normal-ICDW phase transition at $T_{co} \approx 122$ °K.^{9–12} The temperature dependence of the susceptibility above T_{co} may be explained in this case as the behavior of a narrow-band paramagnet (see, however, Ref. 17).

The picture is not clear for the Fe-doped material, however. The low-temperature resistivity minimum has been explained using the concept of the Kondo effect.¹ Negative magnetoresistance and anomalous Hall-constant behavior have been explained using an *s-d* exchange model.^{1,25,26} While a high Kondo-temperature can explain the observed resistivity minimum at T_{min} , the Kondo effect alone does not offer an adequate explanation for experimental findings such as a resistivity maximum at a temperature below T_{min} and a concentration dependent slope of the reduced resistivity versus $\ln T$ curve. It is unlikely that independent localized moments are responsible for such behavior for impurity concentrations of 5% or more.

We note that whenever a system develops a charge-density wave, it is reasonable to presume that the system may show at least an incipient tendency towards spin-density-wave (SDW) formation. The condition for instability against formation of a CDW of wave vector \vec{q} can be written

$$\epsilon(\vec{q}, \omega) = 1 + 4\pi\chi_c(\vec{q}, \omega) = 0, \quad \text{at } \omega = 0,$$

where $\epsilon(\vec{q}, \omega)$ is the longitudinal electronic dielectric function for wave vector q and frequency ω and $\chi_c(\vec{q}, \omega)$ is the corresponding susceptibility. Similarly, the condition for an SDW instability can be written

$$\bar{\mu}(\vec{q}, \omega) = \bar{\Gamma} + 4\pi \bar{\chi}_s(\vec{q}, \omega) = 0 \quad \text{at } \omega = 0,$$

where $\bar{\mu}$ is the electronic-spin permeability tensor and $\bar{\chi}_s$ is the corresponding spin-susceptibility tensor. In simplest approximation, ignoring spin-orbit coupling and using the RPA, χ_c and $\bar{\chi}_s$ are both proportional to the same polarization propagator. Thus those features of the band structure and wave functions which drive a CDW unstable tend also to drive an SDW unstable. This tendency persists in better approximations. We propose therefore that magnetic impurities play a dual role in this material: On the one hand, they reduce the normal-ICDW transition temperature and also smear the transition.^{27,28} On the other hand, they stabilize at the same time an aperiodic modification of a periodic magnetic distortion, a spin-density wave. The first of these two roles is manifested in the susceptibility, for a 2% Fe concentration, as a broadening and shifting to lower temperatures of the sharp maximum seen in the pure material; for a 5% Fe concentration this maximum has completely disappeared. The second of the two roles is manifested by an increase of the susceptibility at low temperatures which, in the 5% Fe concentration, has developed into a pronounced maximum, sensitive to the impurity concentration and the applied external magnetic field. While a Kondo-type mechanism can be responsible for the resistivity minimum, the origin of the maximum is quite different: It is the onset of the SDW which is responsible for the rapid suppression of the spin-flip scattering and, therefore, the formation of a resistivity maximum. Since we expect the temperature derivative of the SDW amplitude to reach its maximum value at T_{SDW} , the temperature at which the SDW first appears, we associate T_{SDW} with the temperature at which the maximum slope in the resistivity versus temperature curve occurs. Following this picture, we expect the susceptibility maximum to occur at T_{SDW} as well, because the presence of the SDW rapidly reduces the existent uniform magnetization. The temperature dependence of the susceptibility of the clean metal above T_{co} is attributed in this picture to an incipient SDW. The CDW is still the dominant instability in this case, responsible for the transition at T_{co} because the SDW needs a finite concentration of magnetic impurities to manifest itself.

In Sec. II we develop a Landau-Ginzburg model to deal with the CDW formation only. Following McMillan¹⁸ we study both the clean material as well as the material doped with nonmagnetic impurities. The first part of Sec. III deals with the formation of

an SDW by generalizing the formalism of Sec. II. We make a random-phase approximation and, therefore, miss the random or spin-glass character of the spin density. The second part contains a model calculation of an impurity-induced SDW in the background of a smeared CDW. Section IV, finally, contains the discussion of our results. In Sec. IV we return to the question of the randomness of the spin density and discuss the interesting possibility of a new type of spin glass associated with a random spin-density wave.

II. CHARGE-DENSITY WAVE FORMATION

The transition-metal dichalcogenides form layered crystal structures in which the basic building block resembles a sandwich with a layer of transition metal between two layers of chalcogen atoms.^{9,13} The layers stack to form the crystal with the metal atom covalently bonded to six chalcogen atoms lying on the corners of either a trigonal prism or an octahedron. These two basic layer forms combine in several ways to form different crystal structures, such as the $2H$, with two layers of chalcogen-metal-chalcogen in a trigonal prismatic coordination and alternate stacking perpendicular to the planes. Each layer is weakly bound to the next, thus forming an anisotropic, mainly two-dimensional crystal. We, therefore, work with a two-dimensional model of charge-density waves (CDW) in one layer, first developed by McMillan.¹⁸ We choose the electron density as the order parameter and, following McMillan, we write down a Landau-Ginzburg free energy in powers of the deviation of the order parameter from its normal value and of its gradients. We perform the calculation more carefully, allowing the amplitude to be complex. Within the random-phase approximation (RPA) which we employ, we find that the minimization of the free energy leads to a set of exact self-consistent equations. We show therefore that the RPA is specifically responsible for the sharp first-order character of the normal to incommensurate CDW transition, as well as for the loss of the impurity pinning mechanism of the CDW.

If $\rho_0(\vec{r})$ is the charge density of the d -band conduction electrons in the normal state, the charge density $\rho(\vec{r})$ is given by

$$\rho(\vec{r}) = \rho_0(\vec{r}) [1 + \alpha(\vec{r})], \quad (2.1)$$

where $\alpha(\vec{r})$ is the real order parameter. It is more convenient to express α in terms of the complex order parameter $\psi_c(\vec{r})$ and its Fourier components around the CDW wave vector \vec{p}_1

$$\alpha(\vec{r}) = \frac{1}{2} [\psi_c(\vec{r}) + \psi_c^*(\vec{r})], \quad (2.2)$$

$$\psi_c(\vec{r}) = \left[\phi_{co} + (A)^{-1/2} \sum_{\vec{q}}' \phi_{c\vec{q}} e^{i\vec{q}\cdot\vec{r}} \right] e^{i\vec{p}_1\cdot\vec{r}}. \quad (2.3)$$

Within the context of a mean-field theory we consider long-wavelength fluctuations only, that is, $\phi_{c\vec{q}}$ appreciably different from zero for $q \ll p_1$. The CDW can have three possible directions \vec{p}_1 because of crystal symmetry. Thus, there are three possible sets of values of ϕ_{c0} and $\phi_{c\vec{q}}$ which require the addition of an index if more than one set is nonzero. However, a single CDW is studied at present, and the free energy is expressed in terms of powers and gradients of $\alpha(\vec{r})$ or $\psi_c(\vec{r})$. The free energy for the clean material has the following contributions per layer:

$$F_C = F_{1C} + F_{2C} \quad (2.4)$$

with

$$F_{1C} = \int d^2r [a_{co}\alpha^2(\vec{r}) + c_{co}\alpha^4(\vec{r})] \quad (2.5)$$

$$F_{2C} = \int d^2r \{ e_{co} [p_1^4 + (\vec{p}_1 \cdot \vec{\nabla})^2] \psi_c(\vec{r})|^2 + f_{co} |\vec{p}_1 \times \vec{\nabla} \psi_c(\vec{r})|^2 \} \quad (2.6)$$

F_{1C} contains the usual Landau terms with a_{co} changing sign at the temperature T_{co} ,

$$a_{co} = a_c'(T - T_{co}) \quad (2.7)$$

The rest of the coefficients do not vary with temperature near the critical temperature. The term F_{2C} is constructed in such a way that (a) the free energy has a minimum when the CDW has the right wave vector \vec{p}_1 and that (b) the free energy does not depend on the direction of the CDW. This term measures the energy it costs the system to distort the charge density from its uniform value.

Using the Fourier expansion for $\psi_c(\vec{r})$ and keeping small q terms only, we obtain the free energy per unit area as a function of ϕ_{c0} , the set $\{\phi_{c\vec{q}}\}$, and the parameters a_{co} , c_{co} , e_{co} , and f_{co} . The fluctuations in the doped material are thermal and impurity driven. Therefore, each $\phi_{c\vec{q}}$ has a random phase associated with it. Thus, we can treat each $\phi_{c\vec{q}}$ as having a random phase, an approximation which is self-consistent in the presence of impurities, and keep only those terms which would survive averaging over the random phases, these being the dominant terms in the sum. The analysis is greatly simplified but we lose the possibility of dealing explicitly with pinning of the phase and amplitude of the charge-density wave by the impurities.

Minimization with respect to the $\phi_{c\vec{q}}$'s leads to a homogeneous system of equations which possesses only the trivial solution $\phi_{c\vec{q}} = 0$. Minimization with respect to ϕ_{c0} gives

$$(g_c + 3|\phi_{c0}|^2)\phi_{c0} = 0 \quad (2.8)$$

where

$$g_c = a_{co}/c_{co} \quad (2.9)$$

For $T > T_{co}$, g_c is positive and only $\phi_{c0} = 0$ is a solution to Eq. (2.8). This corresponds to the normal phase, above the transition temperature, with free energy $F_N = 0$. For $T < T_{co}$, however, the solution

$$|\phi_{c0}|^2 = -2g_c/3 \quad (2.10)$$

yields a lower free energy,

$$F_{CDW} = -\frac{1}{6}g_c^2 \quad (2.11)$$

making this phase stable. This solution corresponds to the formation of a charge-density wave of amplitude ϕ_{c0} , the transition being second order. The phase of the CDW is not determined and lies hidden in ϕ_{c0} .

Doping the material with nonmagnetic impurities translates in our formalism into adding an extra term to the free energy to account for the effect of the impurities:

$$F_{3C} = \int d^2r U(\vec{r}) \rho_0(\vec{r}) \alpha(\vec{r}) \quad (2.12)$$

We expand the impurity potential as we did for $\psi_c(\vec{r})$,

$$V(\vec{r}) = U(\vec{r}) \rho_0(\vec{r}) = \sum_l u_0 \delta(\vec{r} - \vec{r}_l) \quad (2.13)$$

$$V(\vec{r}) = \left[V_0 + (A)^{-1/2} \sum_{\vec{q}} V_{\vec{q}} e^{i\vec{q} \cdot \vec{r}} \right] e^{i\vec{p}_1 \cdot \vec{r}} + \text{c.c.} \quad (2.14)$$

Minimizing again with respect to $\{\phi_{c\vec{q}}\}$ and ϕ_{c0} we obtain a set of equations which becomes exact in the limit of infinite layer area, within the random-phase approximation. This system is solved numerically for each value of the impurity concentration and temperature and the free energy of the normal, as well as the ICDW, state is thus obtained. We find that the transition temperature T_c is suppressed with a square-root-law dependence on the impurity concentration η_c (Fig. 1),

$$T_c = T_{co} - K(C_c)^{1/2} \quad (2.15)$$

where

$$C_c = \frac{\eta_c u_0^2}{16\pi C_{co} p_1^4 (e_{co} f_{co})^{1/2}} \quad (2.16)$$

This rapid reduction of the transition temperature for small impurity concentrations is expected, because even a small number of impurities is enough to destroy the phase correlation of the CDW, thus drastically suppressing T_c . The specific functional dependence, however, may not survive in a microscopic calculation.

We also find the transition to be first order, confirming McMillan's result.¹⁸ The following new features should be noted, however: (a) The assumption of a real ϕ_{c0} is unnecessary and restricts the phase of the CDW. This phase cannot be defined ab-

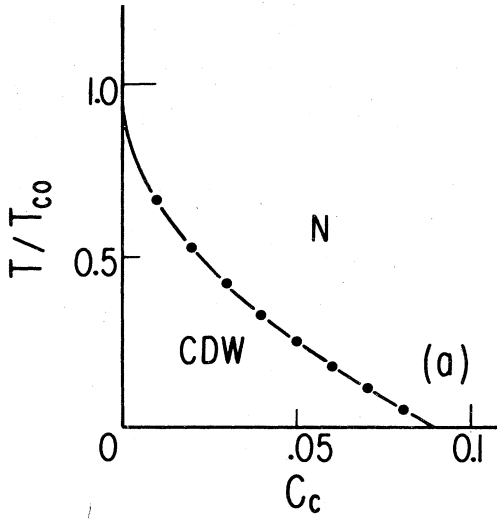


FIG. 1. (a) Normal to ICDW transition temperature vs nonmagnetic impurity concentration. C_c is a dimensionless quantity proportional to the impurity concentration.

solutely, because the mean-field and RPA approximations restore translational invariance so that the free energy becomes independent of this phase. (b) We emphasize the reduction of the transition temperature with increasing impurity concentration, a result which will prove to be important for the formulation of an impurity-induced SDW in the presence of a smeared CDW. (c) The treatment of the CDW formation in the clean material can be generalized, and it will be used in the analysis of the formation of an SDW.

III. MAGNETIC IMPURITIES AND SPIN-DENSITY-WAVE FORMATION

In the first part of this section we examine the possibility for the development of a spin-density wave (SDW), while in the second part we develop a model calculation of an impurity-induced SDW in the background of a smeared CDW, and compare the available experimental data with our results.

A. Is an SDW possible?

The order parameter in this case is the spin density $\vec{m}(\vec{r})$, a vector order parameter. We proceed by generalizing the method of Sec. II to deal with such an order parameter. We concentrate our attention

first on the SDW and ignore the presence of the CDW

$$\vec{m}(\vec{r}) = \frac{1}{2} [\vec{\psi}_s(\vec{r}) + \vec{\psi}_s^*(\vec{r})] , \quad (3.1)$$

$$\vec{\psi}_s(\vec{r}) = \left[\vec{\phi}_{s0} + (A)^{-1/2} \sum_{\vec{q}} \vec{\phi}_{s\vec{q}} e^{i\vec{q}\cdot\vec{r}} \right] e^{i\vec{p}_1\cdot\vec{r}} , \quad (3.2)$$

$$F_S = F_{1S} + F_{2S} + F_{3S} + F_{4S} , \quad (3.3)$$

$$F_{1S} = \int d^2r [a_{s0} \vec{m}^2(\vec{r}) + c_{s0} (\vec{m}^2(\vec{r}))^2] , \quad (3.4)$$

with

$$a_{s0} = a_s'(T - T_{s0}) , \quad (3.5)$$

$$F_{2S} = \int d^2r \sum_l J(\vec{r} - \vec{r}_l) \vec{S}_l \cdot \vec{m}(\vec{r}) , \quad (3.6)$$

$$F_{3S} = \int d^2r \sum_{i=1}^3 \{ e_{s0} | [p_1^4 + (\vec{p}_1 \cdot \vec{\nabla})^2] \psi_s'(\vec{r})|^2 + f_{s0} | \vec{p}_1 \times \vec{\nabla} \psi_s'(\vec{r})|^2 \} , \quad (3.7)$$

$$F_{4S} = \sum_l a_{sl} \vec{S}_l^2 . \quad (3.8)$$

The following should be noted with respect to the various contributions to F_S : The terms F_{1S} and F_{3S} are not different from the corresponding terms previously considered. The term F_{2S} describes the interaction between the spin-density and the thermodynamic variables \vec{S}_l describing the impurity spins. The interaction $J(\vec{r} - \vec{r}_l)$ is Fourier decomposed around the SDW wave vector \vec{p}_1 ,

$$J(\vec{r} - \vec{r}_l) = j_0 \delta(\vec{r} - \vec{r}_l) = \left[J_0 + (A)^{-1/2} \sum_{\vec{q}} J_{\vec{q}} e^{i\vec{q}\cdot(\vec{r} - \vec{r}_l)} \right] e^{i\vec{p}_1\cdot(\vec{r} - \vec{r}_l)} + \text{c.c.} \quad (3.9)$$

The F_{4S} contribution, finally, is analogous to the contribution of the usual magnetization in a magnetic system. The calculation proceeds as for the CDW case. The use of the RPA in obtaining the magnetic part of the free energy destroys the correlation between the phase and amplitude of the spin density and the positions of the magnetic impurities. The impurity spin itself is a dynamic variable, too, since its orientation is not predetermined. Both the spin-density and the impurity moment change to find the point of minimum energy.

Accordingly, the free energy is minimized now with respect to both the impurity spin variables \vec{S}_l and the Fourier components $\vec{\phi}_{s\vec{q}}$ of the spin density. This procedure leads to a homogeneous system of

equations, which accepts only the trivial solution. The free energy thus takes the form

$$F_S = \frac{1}{2}(g_s - C_s) |\bar{\phi}_{s0}|^2 + \frac{1}{8} [\bar{\phi}_{s0}^2 \bar{\phi}_{s0}^{*2} + 2(\bar{\phi}_{s0} \cdot \bar{\phi}_{s0}^*)^2] , \quad (3.10)$$

where C_s is a dimensionless quantity proportional to the impurity concentration, η_s ,

$$C_s = \frac{\eta_s j_0^2}{2a_{s1}c_{s0}} \quad (3.11)$$

and

$$g_s = a_{s0}/c_{s0} . \quad (3.12)$$

For $g_s - C_s > 0$ the minimum free energy occurs at $\bar{\phi}_{s0} = 0$, corresponding to the normal state. For $g_s - C_s < 0$ nonzero solutions exist corresponding to the SDW state. The condition $g_s - C_s = 0$ connects the transition temperature T_s with the impurity concentration η_s

$$T_s = T_{s0} + \frac{j_0^2}{2a_{s1}a_s} \eta_s . \quad (3.13)$$

A similar calculation, second order in the $\bar{\phi}_{s\bar{q}}$'s, gives at the minimum free energy

$$(\epsilon_{s\bar{q}} - \frac{1}{2}C_s) \bar{\phi}_{s\bar{q}} = 0 , \quad (3.14)$$

where,

$$\epsilon_{s\bar{q}} = \frac{1}{2}g_s + \frac{e_{s0}}{c_{s0}} \{p_1^4 - [\bar{p}_1 \cdot (\bar{p}_1 + \bar{q})]^2\} + \frac{f_{s0}}{c_{s0}} (\bar{p}_1 \times \bar{q})^2 . \quad (3.15)$$

Equation (3.14) relates the susceptibility of the doped material, $\chi_{\bar{q}}$, to the susceptibility of the clean material, $\chi_{\bar{q}}^0$, and the susceptibility of the impurities, χ_I ,

$$\chi_{\bar{q}} = \frac{\chi_{\bar{q}}^0}{1 - \eta_s j_0^2 \chi_I \chi_{\bar{q}}^0 / c_{s0}} . \quad (3.16)$$

Thus, a direct consequence of the magnetic impurities is the enhancement of the susceptibility, as is seen from Eq. (3.16). This enhancement is a maximum for $q = 0$ and is the origin of the transition temperature increase.

The enhancement of the transition temperature increases with increasing impurity concentration. This characteristic of the SDW formation is caused by the dynamic character of the impurity moments. The more impurities, the easier it is for the SDW to form, because the local magnetic field orients the magnetic moments creating a constructive feedback mechanism that reinforces its buildup. This is to be contrasted

with the CDW formation, where the wave is forced to distort itself, adjusting to the impurity potential. The more impurities there are, the more difficult it becomes for the CDW to satisfy the local impurity potential constraints, without raising at the same time the kinetic energy. We isolate here the origin of the competition between the charge and the spin-density waves. As the impurity concentration η increases, there exists a critical concentration η^* such that for $\eta < \eta^*$ the CDW wins over the SDW, while for $\eta > \eta^*$ it is the SDW that dominates (Fig. 2). The role of the impurities is to destabilize the CDW while stabilizing simultaneously the SDW.

The formalism developed above includes the effect of indirect impurity interactions. In the present calculation the impurity spin variables \bar{S}_i were eliminated in favor of the Fourier components $\bar{\phi}_{s\bar{q}}$ and these in turn were eliminated in favor of $\bar{\phi}_{s0}$. Alternatively, the spin-density variables $\bar{\phi}_{s\bar{q}}$ and $\bar{\phi}_{s0}$ could have been eliminated in favor of the impurity spin variables \bar{S}_i . In that case the form of the free energy would have emerged containing impurity spin interactions, ultimately equivalent to Eq. (3.10). The interactions, however, are indirect and intermediated by the conduction electrons. They do not include direct interactions between the impurities which would presumably be ferromagnetic in character. These have been omitted because, as will appear later in this section, we are concerned with compositions Fe_xTaSe_2 for $x \leq 0.1$. At such concentrations, the mean separation of the Fe atoms is too large for the direct interaction to be important. At much higher concentrations, around 30%, a ferromagnetic state is indeed stabilized but we do not address that situation here.

In order to examine the case where both a charge- and a spin-density wave can form, we introduce an

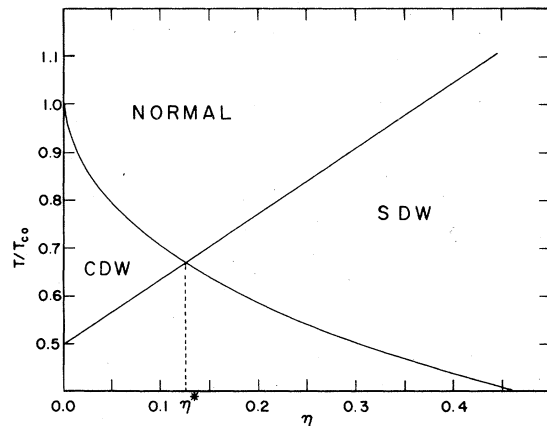


FIG. 2. Normal to ICDW and normal to SDW transition temperatures vs impurity concentration, to demonstrate the competition between the two instabilities.

interaction term in the free energy

$$F_{INT} = g \int d^2r \alpha^2(\vec{r}) \bar{m}^2(\vec{r}) . \quad (3.17)$$

The calculations proceed within the framework of the approximations already discussed. We examine two physical situations

1. Clean material

Let $\phi_{s0}^i = P_i e^{i\theta_i}$ and $\phi_{c0} = R e^{i\phi_c}$. The minimization procedure then leads to four possible solutions, where $R \neq 0$ and $P_i \neq 0$, $i = 1, 2, 3$. Namely,

$$\theta_1 = \theta_2 = \theta_3 = \phi_c , \quad (a)$$

$$\theta_1 = \theta_2 = \theta_3 = \phi_c - \frac{1}{2}\pi , \quad (b)$$

$$\theta_1 = \theta_2 = \theta_3 + \frac{1}{2}\pi = \phi_c \quad (c)$$

and

$$\theta_1 = \theta_2 = \theta_3 + \frac{1}{2}\pi , \quad \phi_c = \theta_1 + \frac{1}{2}\pi . \quad (d)$$

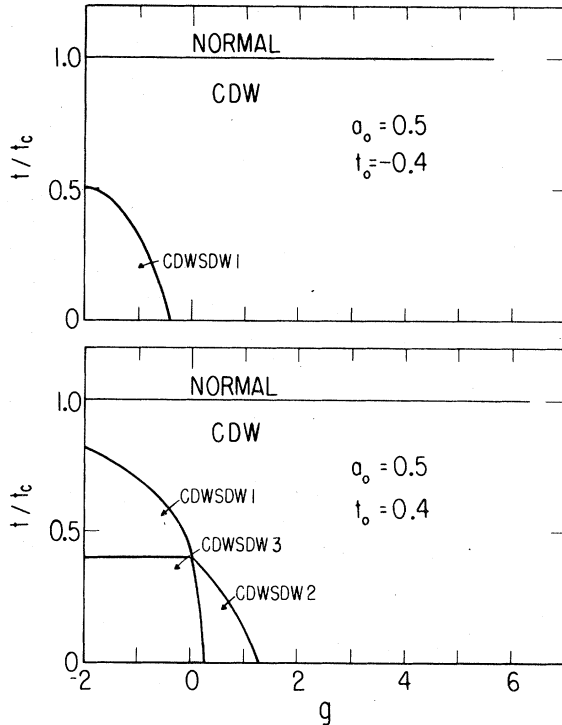


FIG. 3. Phase diagram for the clean material ($C_s = 0$), in the temperature-coupling constant space. The symbols CDWSDW1, CDWSDW2, etc. correspond to cases (a) through (d) (see Sec. III A). To reduce the number of existing parameters, we take $c_{c0} = c_{s0}$, $a_0 = a_{s0}/a_{c0}$, and with

$$t = \frac{a_{c0} T}{c_{c0}} , \quad t_c = \frac{T_{c0} a_{c0}}{c_{c0}} , \quad t_0 = \frac{T_{s0} a_{c0}}{c_{c0}} ,$$

we have $g_c = t - t_c$ and $g_s = a_0(t - t_0)$. The coupling constant g is also normalized with respect to c_{c0} .

For each value of the temperature the free energy of the normal, the CDW, the SDW, and the CDWSDW state is calculated. By varying the temperature and the coupling constant g we obtained the phase diagram in the T - g plane (Fig. 3). This diagram determines the physically relevant range of values for the coupling constant g , for no SDW is observed experimentally in the clean metal.

2. Doped material

Magnetic impurities interact, in general, with both the spin and the charge densities. The minimization equations form, in this case, a highly nonlinear system of complex equations, impossible to solve. We examined the case of magnetic interactions alone and the case of weak coupling between the Fourier components $\phi_{c\vec{q}}$ and $\phi_{s\vec{q}}$, in which the solutions could be determined numerically. The phase diagrams so obtained revealed that the crossover indeed occurs, and that the character of the instability changes as we move past this particular point. Examples, in the T - C_s plane, are presented in Fig. 4. Thus, competition between the two instabilities is possible, supporting our physical picture.

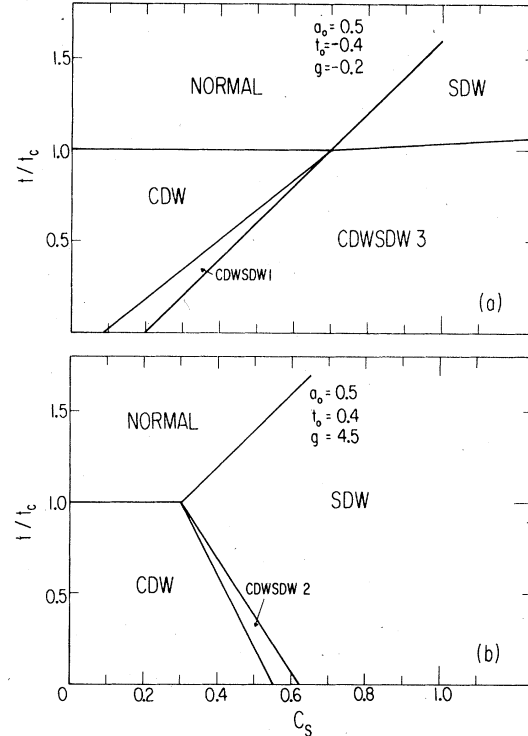


FIG. 4. Phase diagrams of the doped material. The magnetic interaction only is taken into account. The symbols CDWSDW1, CDWSDW2, etc. correspond to cases (a) through (d) (see Sec. III A). The normalization is the same as in Fig. 3 and C_s is a dimensionless parameter proportional to the impurity concentration (see text).

B. Model calculation of an impurity-induced SDW

We turn our attention now to developing a model for the interpretation of the experimental findings on iron intercalated into $2H\text{-TaSe}_2$ ($2H\text{-Fe}_x\text{TaSe}_2$) based on a CDW to CDWSDW transition. We know that there is a CDW in pure $2H\text{-TaSe}_2$ which persists in the presence of intercalated Fe impurities. We know also that there are magnetic anomalies at low temperatures which indicate that intercalated Fe possesses a local moment and yet which differ from what is to be expected from direct interaction among the Fe atoms. We can argue that an unrealized or suppressed tendency towards SDW formation can occur in pure $2H\text{-TaSe}_2$ on the basis of the discussion in the introduction and the calculations of Sec. III A. Accordingly, we propose that the Fe, acting as magnetic impurities, stabilize the SDW in the manner described in Sec. III A and attribute the magnetic anomalies to a CDW to CDWSDW phase transition.

We have seen from our analysis in Secs. II and III A that impurities tend to suppress the CDW, whereas magnetic impurities enhance a stable SDW and stabilize or induce a marginally unstable one. This reduction of T_c and raising of T_s opens the question of whether there is interference between the two instabilities, which would complicate the analysis given in this section. A careful analysis shows that impurities destroy long-range order, causing the smearing of the transition associated with the CDW formation.^{27,28} Indeed, the temperature of the normal-ICDW phase transition is reduced and the transition smeared in the $x = 0.005$ and $x = 0.02$ samples.⁷ In the 0.5% case the susceptibility maximum occurs at $T_c \approx 116^\circ\text{K}$ and is still relatively sharp. The 2% sample shows a broad maximum at a temperature between 100 and 110 °K. We use this information together with Eq. (2.15) to estimate the temperature range for the development of the CDW in the 10% sample, which has the largest iron concentration studied. The normal-ICDW transition temperature is estimated to be in the 95 °K temperature region. Thus, the CDW is fully developed and its amplitude is nearly temperature independent in the temperature range in which the pronounced susceptibility maximum occurs, for all concentrations of interest. Its main effect, therefore, is to modify the parameters of the free energy associated with the magnetic variables in an almost temperature-independent manner. Accordingly, we suppose there to be no interference between the CDW and the CDWSDW transitions and ignore the explicit contribution of the CDW to the free energy.

The susceptibility curves exhibit also a dramatic increase at low temperatures, even at 0.5% Fe concentration. We attribute this increase to the onset of the magnetic-impurity-induced SDW. We note that even in the clean material the susceptibility shows a slight

increase as the temperature approaches zero,¹⁷ which is consistent with the existence of an incipient SDW. Accordingly, we describe these systems in terms of a Landau-Ginzburg free energy, which contains the following contributions per layer:

$$F_1 = \frac{1}{2} a_1 (T - T_{so}) P^2 + \frac{1}{4} b_1 P^4 + \frac{1}{2} a_2 M^2 + \frac{1}{4} b_2 M^4 + \frac{1}{2} c M^2 P^2, \quad (3.18)$$

$$F_2 = \frac{J_0}{A} \sum_l (M S_l + P S_l \cos \bar{p}_1 \cdot \bar{r}_l), \quad (3.19)$$

$$F_3 = \frac{a_s T}{2A} \sum_l S_l^2 + \frac{b_s}{A} \sum_l S_l^4, \quad (3.20)$$

$$F_{SH} = -MH - \frac{1}{A} \sum_l S_l H, \quad (3.21)$$

$$F = F_1 + F_2 + F_3 + F_{SH}, \quad (3.22)$$

where P is the amplitude of the SDW, M the uniform magnetization induced by the applied magnetic field H , S_l the impurity spin variable, and A the area of the layer. We choose T_{so} , the transition temperature associated with SDW formation, to be negative because no SDW is observed in the clean metal: either the SDW is unstable or it is suppressed by a repulsive interaction with the CDW. In either case the effective transition temperature for the development of the SDW is negative in the absence of magnetic impurities.

When the SDW develops, a substantial mean magnetic moment also develops for each impurity atom. While it was sufficient for the location of phase boundaries to ignore the fourth-order terms in the impurity spins, it is necessary to include them and the temperature dependence of the impurity spin susceptibility in the present section in order to describe the system below the magnetic transition temperature. In their absence, it is a trivial matter to eliminate the impurity spins \bar{S}_l in terms of $\bar{M}(\bar{r})$. In their presence, the mean-field equations become so difficult to solve that it is necessary to abandon hope of describing the polarization of the SDW accurately and keep only that component of each spin order parameter parallel to the applied field. Since we are not concerned with the pinning of the wave, we extract the $q = 0$ and $q = p_1$ Fourier components from the impurity spin variables

$$S_l = S_1 + S_2 \cos \bar{p}_1 \cdot \bar{r}_l. \quad (3.23)$$

We thus have a four order-parameter model, these being P , M , S_1 , and S_2 (note that S_1 also goes to zero as H goes to zero). We employ again a random-phase approximation when evaluating the terms that contain powers of $\cos(\bar{p}_1 \cdot \bar{r}_l)$. The free energy is then minimized and the resulting equations are solved numerically to determine the four order parameters. We calculate in this way the total uniform magnetization $S_T = M + \eta S_1$, η being the im-

purity area density and both the differential bulk susceptibility $\chi = (\partial S_T / \partial H) / (\rho h)$ and the ratio $\chi' = (S_T / H) / (\rho h)$, where ρ is the density of the material and h is the height of the unit cell, measured with the same unit length.

For $H = 0$ the transition temperature for the onset of the SDW can be calculated analytically

$$T_S(H=0) = \frac{1}{2} T_{s0} + \left[\left(\frac{1}{2} T_{s0} \right)^2 + \frac{\eta J_0^2}{2 a_1 a_s} \right]^{1/2}. \quad (3.24)$$

The difference between Eqs. (3.24) and (3.13) arises from making the Curie-like temperature dependence of the impurity spin susceptibility explicit by the use of $\frac{1}{2} a_s T$ in Eq. (3.20) in place of a_{sT} in Eq. (3.8).

For negative T_{s0} , $T_S(0)$ is positive for any finite impurity concentration. When the magnetic field is turned on, this temperature decreases (Fig. 5), because the field tends to orient the impurity spins in its direction, thus reducing their oscillatory orientation. The S_T/H curves (Fig. 6) reveal the following: (a) the magnitude of the maximum decreases with increasing magnetic field, (b) the temperature T_{\max} of the maximum also decreases with increasing H , and (c) there is an asymmetry in the susceptibility above and below T_{\max} , i.e., the susceptibility drops much faster below T_{\max} than it does above. All of these features are observed experimentally⁷ and can be understood in terms of SDW formation: The maximum occurs at the onset of the SDW, which forces a reduction of the uniform magnetization. We

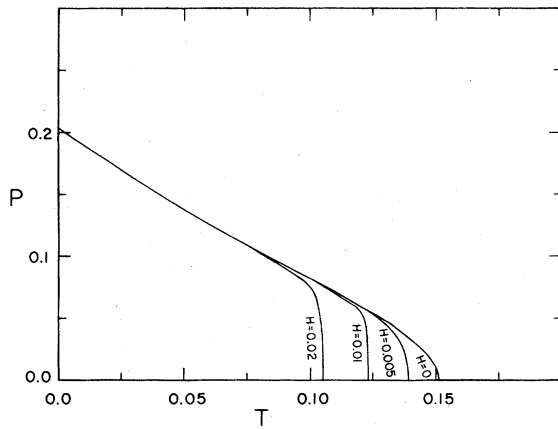


FIG. 5. Temperature dependence of the amplitude of the SDW. The free energy is scaled so that all quantities involved are pure numbers. The numerical values of the coefficients are:

$$\begin{aligned} a_1 &= 0.8, & a_2 &= 0.6, & a_s &= 1.5, & b_1 &= 0.4, \\ b_2 &= 0.8, & b_s &= 0.6, & c &= 0.6, & J_0 &= 0.8, \\ \eta &= 0.2, & T_{s0} &= -0.2. \end{aligned}$$

The magnetic field is symbolized by H .

identify, therefore, T_{\max} with $T_S(H)$ and explain in this way the suppression of T_{\max} with increasing H . The steep slope of the SDW amplitude, as a function of temperature, near $T_S(H)$ is reflected in the fast drop of the S_T/H vs T curve, below T_{\max} . Since we eliminate the spatial randomness of the impurity spins by employing the RPA and ignore the possibility of randomness in their orientation and in the orientation of the spin density, it is not surprising that the calculated curves have a cusp and not the observed rounded maximum, for finite H .

For high temperatures and low fields the bulk susceptibility becomes

$$\chi' = \frac{1}{\rho h a_2} + \frac{\eta(1 - J_0/a_2)^2}{a_s \rho h [T - (\eta J_0^2 / a_2 a_s)]}. \quad (3.25)$$

The high-temperature susceptibility obeys, therefore, a Curie-Weiss law

$$\chi' = \chi_0 + \frac{C_1}{T - \theta} \quad (3.26)$$

with χ_0 , C_1 , and θ appropriately defined from Eq. (3.25). The constant C_1 can be rewritten in terms of an effective magnetic moment μ_{eff} ,

$$C_1 = \frac{N_i \mu_{\text{eff}}^2}{3 K_B \rho}, \quad (3.27)$$

where $N_i = \eta/h$ is the impurity concentration. This moment in turn can be expressed in terms of the free-impurity moment μ_0 ,

$$\mu_{\text{eff}} = \mu_0 \left| 1 - \frac{J_0}{a_2} \right|. \quad (3.28)$$

We have fitted Eq. (3.26) to the high-temperature region of the susceptibility data for the $x = 0.05, 0.08$, and 0.10 samples. Table I contains the results of these fittings. Our model predicts that θ should increase linearly with increasing impurity concentration and that μ_{eff} should be concentration independent.

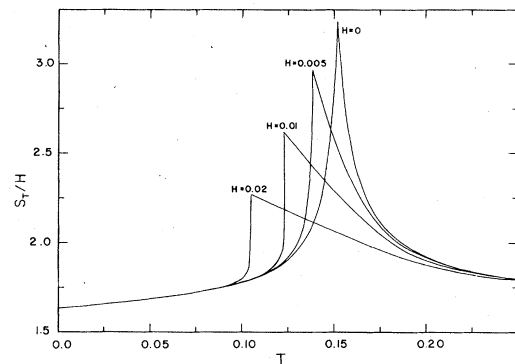


FIG. 6. Temperature dependence of the ratio S_T/H . The conditions of Fig. 5 apply also here.

TABLE I. Values of the parameters χ_0 , μ_{eff} , and θ , obtained from the high-temperature fittings of the susceptibility data of Ref. 7.

x	$\chi_0(10^{-6} \text{ emu/g})$	$\mu_{\text{eff}}(\mu_B)$	θ ($^\circ\text{K}$)
0.05	0.62	2.87	1
0.08	0.62	2.94	7
0.10	0.79	3.61	20

While θ does increase with increasing Fe concentration, its dependence on the latter deviates from linearity. Similarly, μ_{eff} shows a weak concentration dependence. In both cases the values extracted from the fittings are smaller than the predicted ones. This is a consequence of the presence of the smeared CDW, which is left out of our model. The background susceptibility contains many contributions, which become a source of ambiguity in determining the parameter a_2 . This parameter contains the Pauli contribution only and does not take into account such contributions as the Landau diamagnetism, the Ta and Se cores diamagnetism, and the Van Vleck paramagnetism. Nevertheless, ignoring this and using the χ_0 value extracted from the 10% data, we get

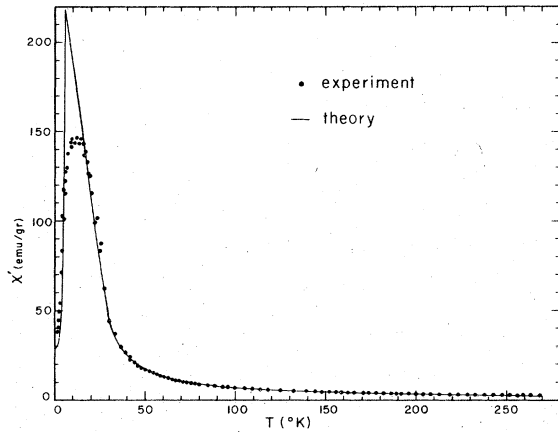


FIG. 7. Numerical fit of the 10% susceptibility data of Ref. 7. The estimated parameters are:

$$\begin{aligned}
 a_1 &= 4.8 \times 10^1 \text{ deg}^{-1} \text{ \AA}^{-1}, & a_2 &= 2.3 \times 10^4 \text{ \AA}^{-1}, \\
 a_3 &= 2.7 \times 10^{-1} \text{ deg}^{-1} \text{ \AA}^{-3}, & b_1 &= 1.5 \times 10^{10} \text{ eV}^{-1}, \\
 b_2 &= 1.5 \times 10^{10} \text{ eV}^{-1}, & b_3 &= 1.6 \times 10^6 \text{ eV}^{-1} \text{ \AA}^{-6}, \\
 c &= 9.0 \times 10^9 \text{ eV}^{-1}, & J_0 &= 3.5 \times 10^3 \text{ \AA}^{-1}, \\
 \eta &= 9.8 \times 10^{-3} \text{ \AA}^{-2}, & T_{30} &= -240 \text{ }^\circ\text{K}.
 \end{aligned}$$

for the free-iron moment $\mu_0 = 4.3 \mu_B$, compared to $4.9 \mu_B$ for the spin part of Fe^{2+} (μ_B is the Bohr magneton). The value of μ_0 increases as we increase χ_0 , which suggests that the Pauli contribution is indeed larger than the χ_0 we get from the fitting. Since μ_{eff} is smaller than the magnetic moment of either ferrous or ferri ions, we conclude that J_0 is positive, which implies an antiferromagnetic coupling between the impurity spins and the spin density. We have also used our model to fit the susceptibility data of the 10% sample, in both the high- and the low-temperature regions. The results of this fitting are presented in Fig. 7. The quality of the fit is quite good, considering the limitations of the mean-field and RPA approximations and the simplifying assumptions introduced in the course of developing this model.

Hall-constant measurements show remarkable non-linear dependence on the applied magnetic field and temperature,^{1,2,7} reminiscent of the extraordinary component observed in ordered magnetic systems and in spin glasses.²⁹⁻³¹ In the presence of an internal field the Hall coefficient R_H is given by

$$R_H = R_0 + 4\pi R_s [S_T(H)/H], \quad (3.29)$$

where R_0 is the normal Hall coefficient, R_s the spontaneous Hall coefficient, H the applied magnetic field, and $S_T(H)$ the total magnetization.^{32,33} Measurements of the temperature dependence of the Hall resistivity and Hall constant indicate that their behavior is very much like that of χ .² We have applied our model to obtain the field dependence of the ratio S_T/H . The results are presented in Fig. 8. They show the characteristic nonlinear behavior of the experimental data.^{1,2,7}

At this point, we employ our model in order to understand the observed anomalies in the resistivity

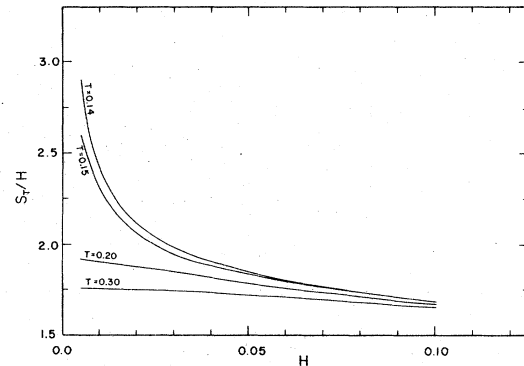


FIG. 8. Field dependence of the ratio S_T/H , for different temperatures, to demonstrate the nonlinear behavior of the Hall coefficient (see text). The conditions of Fig. 5 apply also here.

and magnetoresistance data. The resistivity has a Kondo-like minimum accompanied by a maximum at a lower temperature.^{1,2} We note first that the conventional Kondo effect, involving isolated localized impurity moments, cannot account for the resistivity features. The reduced resistivity versus $\ln T$ plots possess a concentration dependent slope,¹ not expected in a traditional Kondo system. Furthermore, the impurity moments cannot be treated as isolated, in view of the fact that in an ideal, two-dimensional, substitutional, hexagonal, binary alloy containing 10% solute ions, only 53% of them have no nearest neighbor of the same kind (the percentage becomes 28% for a three-dimensional fcc structure). We conclude, therefore, that for iron concentrations of about 5% and more the simple Kondo mechanism should be disregarded as the dominant mechanism for the resistivity minimum. Nonuniformly distributed iron atoms can, however, cause a Kondo-like behavior, the magnetic moments being associated with groups of iron atoms rather than individual atoms. The observed logarithmic temperature dependence of the resistivity near the minimum points in the direction of a Kondo-type mechanism (though not necessarily the conventional one). While such a generalized Kondo effect can account for the minimum, the observed maximum is still unaccounted for. We employ the physical picture already developed, attributing this maximum to the reduction of spin-flip scattering.³⁴⁻³⁷ Two mechanisms can be responsible for this reduction: either an external magnetic field is applied or an internal field is present. In either case the field locks the impurity spins in its direction, reducing in this way spin-flip scattering. The first mechanism is responsible for the negative magnetoresistance. The stronger the field the more spin-flip-scattering suppression it causes, and the more the magnetoresistance decreases. The second mechanism is responsible for the anomalous behavior of the resistivity and magnetoresistance curves. Because the rate at which the SDW amplitude increases with decreasing temperature is maximum at T_{\max} , we identify T_{\max} with the temperature of maximum slope in the resistivity versus T plots. The experiments seem to support this interpretation,^{1,2} even though measurements looking specifically for this correlation do not yet exist. Finally, SDW formation can account for the field and temperature dependence of the magnetoresistance. For small applied fields and low temperatures (below T_{\max}) the interplay between the external magnetic field and the internal fields created by the SDW enhances spin-flip scattering, thus increasing the magnetoresistance. When the applied field is large enough or if the temperature is above T_{\max} , the magnetoresistance decreases with increasing field. For $T < T_{\max}$, therefore, the negative magnetoresistance should exhibit a minimum for small fields, while for $T > T_{\max}$ this minimum should

disappear and the negative magnetoresistance should increase with increasing field, for all values of the field. This behavior too is observed experimentally.^{1,2}

IV. DISCUSSION

Within the framework of a Landau-Ginzburg mean-field theory we find that magnetic impurities in $2H\text{-TaSe}_2$ tend to suppress the CDW formation, while enhancing the formation of an SDW. Various phases show up in the phase diagrams and, depending upon the choice of the parameters of the model, the SDW or the CDWSDW state may be the stable one at low temperatures (see for example Figs. 3 and 4). However, as discussed in Sec. III B, the experiments indicate that the impurities stabilize an aperiodic modification of the SDW, with a smeared CDW serving as background.

The essential features of the experimental data are correctly predicted, even within the limitations of the mean-field theory. Namely, (a) the rapid drop of the susceptibility with decreasing temperature below T_{\max} and its correct high-temperature behavior; (b) the lowering of T_{\max} with increasing magnetic field; (c) the sharpening of the susceptibility maximum with decreasing H ; (d) the correct nonlinear dependence on the temperature and the magnetic field of the Hall coefficient, for different iron concentrations; (e) the observed resistivity maximum at low temperatures; and (f) the field and temperature dependence of the observed negative magnetoresistance.

While this success is an indication that the correct physical idea is incorporated into our model, on the other hand, the present calculation omits (a) the random nature of the phase of the SDW, associated with the random spatial distribution of the magnetic impurities, by employing the random-phase approximation. Thus, we omit the pinning of the wave and the loss of long-range order.

(b) Our calculation does not take into account the possible random orientation of the SDW and the impurity spins: we simplified the free energy in Sec. III B by assuming that

$$S_x = S_y = 0, \quad P_x = P_y = 0, \quad S_z \neq 0, \quad P_z \neq 0.$$

The detailed calculations underlying the results of Sec. III A reveal that the SDW developing is a spiral one with its axis of rotation arbitrarily oriented with respect to the direction of propagation. This degeneracy raises the possibility that one may have a locally defined spiral SDW, with its axis of rotation changing randomly in space. Even if such a spiral SDW is not actually realized and the material favors the development of a linear SDW, the fact that more than one SDW may be present, raises the possibility of an SDW possessing a wave vector \vec{p}_1 in one region of space and a different wave vector \vec{p}_2 in another, thus

adding again orientational randomness to this already complex random system. (c) Finally, we omit fluctuations of the order parameter by employing the mean-field approximation.

The inclusion of (c) results mostly in quantitative changes. The inclusion of (a) and (b) would give rise to a novel kind of spin-glass state: The conventional spin-glass system consists of localized magnetic moments on a set of impurities, randomly distributed in a nonmagnetic host.³⁸⁻⁴² There exists also a second kind of spin glass, known as the Stoner glass, consisting of diffuse magnetic moments associated with random impurities in a nearly magnetic host.⁴³ A third possible kind, suggested by the present work, consists of localized magnetic moments and a random SDW in a nearly magnetic host. We call it a "spin-density-wave glass". The experimental data provide some evidence that orientational, as well as spatial randomness exists: magnetization versus magnetic field measurements exhibit a hysteresis loop,⁷ characteristic of such a state. It would be interesting to see if the sharpening of the pronounced maximum in the susceptibility extrapolates to a cusp in the limit of zero field. The experimental technique used in Ref. 7 already distinguishes between the spin-density-wave glass and the conventional spin glass. In the latter, the magnetization reaches its maximum value at zero temperature, as the temperature is lowered, in the presence of a constant magnetic field.⁴⁴ In the former, the magnetization drops suddenly at T_{\max} during such a field-cooling experiment, because it is reduced by the development of the SDW. It would be in-

teresting to compare the behavior of these two systems with increasing temperature, after zero-field cooling.

Even though the available experimental data support the development of an SDW in our system, a direct proof of its existence does not, at present, exist. We wish, therefore, to suggest that neutron scattering experiments be performed in these systems (e.g., Fe-doped $2H\text{-TaSe}_2$), in order to detect the development and stabilization of the SDW phase, as the temperature is lowered. In support of our model we point to the fact that we reproduce correctly the observed anomalous behavior of the susceptibility and Hall-constant data, in a semiquantitative way, within the mean-field theory we employ and that we explain qualitatively the peculiar features of the resistivity and magnetoresistance measurements. The present phenomenological calculation, however, does not account quantitatively for the details of these measurements. It offers instead a clear physical picture which can serve as the basis for calculations that go beyond the mean-field theory.

ACKNOWLEDGMENTS

The author expresses his appreciation and gratitude to Professor Morrel H. Cohen for suggesting this problem and for his guidance throughout the work, and thanks Dr. R. V. Coleman for use of the experimental data of Ref. 7 prior to their publication. This work was supported by NSF Grant No. DMR77-12637.

*Submitted in partial fulfillment of the requirements for the Ph.D. degree in the Dept. of Phys., the Univ. of Chicago.

- ¹D. A. Whitney, R. M. Fleming, and R. V. Coleman, Phys. Rev. B **15**, 3405 (1977).
- ²D. A. Whitney, R. M. Fleming, and R. V. Coleman, Solid State Commun. **18**, 309 (1976).
- ³F. J. DiSalvo, J. A. Wilson, B. G. Bagley, and J. V. Waszczak, Phys. Rev. B **12**, 2220 (1975).
- ⁴F. J. DiSalvo, J. A. Wilson, and J. V. Waszczak, Phys. Rev. Lett. **36**, 885 (1976).
- ⁵J. J. Hauser, M. Robbins, and F. J. DiSalvo, Phys. Rev. B **8**, 1038 (1973).
- ⁶R. C. Morris, Phys. Rev. Lett. **34**, 1164 (1975).
- ⁷S. J. Hillenius, R. V. Coleman, E. R. Domb, and D. J. Sellmyer, Phys. Rev. B **19**, 4711 (1979).
- ⁸M. H. Van Maaren and G. M. Schaeffer, Phys. Lett. A **24**, 645 (1967).
- ⁹D. E. Moncton, J. D. Axe, and F. J. DiSalvo, Phys. Rev. Lett. **34**, 734 (1975); Phys. Rev. B **16**, 801 (1977).
- ¹⁰J. A. Wilson, F. J. DiSalvo, and S. Mahajan, Adv. Phys. **24**, 117 (1975).
- ¹¹J. M. E. Harper, T. H. Geballe, and F. J. DiSalvo, Phys. Rev. B **15**, 2943 (1977).
- ¹²E. F. Steigmeier, G. Harbeke, H. Auderset, and F. J.

DiSalvo, Solid State Commun. **20**, 667 (1976).

- ¹³J. A. Wilson and A. D. Yoffe, Adv. Phys. **18**, 197 (1969).
- ¹⁴R. A. Craven and S. F. Meyer, Phys. Rev. B (to be published).
- ¹⁵J. A. Wilson, F. J. DiSalvo, and S. Mahajan, Phys. Rev. Lett. **32**, 882 (1974).
- ¹⁶A. H. Thompson, Phys. Rev. Lett. **34**, 520 (1975).
- ¹⁷J. L. Benchimol, F. T. Hedgcock, and F. J. DiSalvo, Solid State Commun. **25**, 677 (1978).
- ¹⁸W. L. McMillan, Phys. Rev. B **12**, 1187 (1975).
- ¹⁹T. M. Rice, Solid State Commun. **17**, 1055 (1975).
- ²⁰W. L. McMillan, Phys. Rev. B **14**, 1496 (1976).
- ²¹G. Campagnoli, A. Gustinetti, and A. Stella, Phys. Rev. Lett. **38**, 95 (1977).
- ²²W. L. McMillan, Phys. Rev. B **16**, 643 (1977).
- ²³W. L. McMillan, Phys. Rev. B **16**, 4655 (1977).
- ²⁴N. J. Doran, B. Ricco, M. Schreiber, D. Titterton, and G. Wexler, J. Phys. C **11**, 699 (1978).
- ²⁵M. T. Béal-Monod and R. A. Weiner, Phys. Rev. **170**, 552 (1968).
- ²⁶R. A. Weiner and M. T. Béal-Monod, Phys. Rev. B **3**, 145 (1971).
- ²⁷L. J. Sham and B. R. Patton, Phys. Rev. B **13**, 3151 (1976).
- ²⁸Y. Imry and S. Ma, Phys. Rev. Lett. **35**, 1399 (1975).

- ²⁹S. P. McAlister and C. M. Hurd, *Solid State Commun.* **19**, 881 (1976).
- ³⁰C. M. Hurd and S. P. McAlister, in *Amorphous Magnetism II*, edited by R. A. Levy and R. Hasegawa (Plenum, New York, 1977).
- ³¹S. V. Vonsovskii, *Magnetism* (Wiley, New York, 1974), Vol. 2, p. 1146.
- ³²C. M. Hurd, *The Hall Effect in Metals and Alloys* (Plenum, New York, 1972), Chap. 5, and references therein.
- ³³For a ferromagnet above the Curie point or a paramagnet $M = \chi H$ and Eq. (4.20) becomes $\rho_H = H(R_0 + 4\pi\chi)$; see also Ref. 30, p. 172.
- ³⁴M. T. Béal-Monod, *Phys. Rev.* **178**, 874 (1969).
- ³⁵K. Matho and M. T. Béal-Monod, *Phys. Rev. B* **5**, 1899 (1972).
- ³⁶O. Laborde and P. Radhakrishna, *J. Phys. F* **3**, 1731 (1973).
- ³⁷O. A. Tindall and M. H. Jericho, *Phys. Rev. B* **9**, 3113 (1974).
- ³⁸V. Cannella and J. A. Mydosh, *Phys. Rev. B* **6**, 4220 (1972).
- ³⁹S. F. Edwards and P. W. Anderson, *J. Phys. F* **5**, 965 (1975).
- ⁴⁰D. Sherrington and B. W. Southern, *J. Phys. F* **5**, L49 (1975).
- ⁴¹K. H. Fisher, *Phys. Rev. Lett.* **34**, 1438 (1975).
- ⁴²D. Sherrington and S. Kirkpatrick, *Phys. Rev. Lett.* **35**, 1792 (1975).
- ⁴³J. A. Hertz, *Phys. Rev. B* **19**, 4796 (1979).
- ⁴⁴P. A. Beck, *Met. Trans.* **2**, 2015 (1971).